

Compound figure of merit for photonic applications of metal nanocomposites

Hernando Garcia^{a)}

Department of Physics, Southern Illinois University, Edwardsville, Illinois 62026

Hare Krishna and Ramki Kalyanaraman

Department of Physics, Washington University in St. Louis, St. Louis, Missouri 63130

(Received 9 June 2006; accepted 12 August 2006; published online 3 October 2006)

Selecting nanocomposites for photonic switching applications requires optimizing their thermal, nonlinear, and two-photon absorption characteristics. The authors simplify this step by defining a compound figure of merit (FOM_C) for nanocomposites of noble metals in dielectric based on criteria that limit these structures in photonic applications, i.e., thermal heating and two-photon absorption. The device independent results predict extremely large values of FOM_C for a specific combination of the metal and insulator dielectric constants given by $\epsilon_h = (\epsilon_1 - \epsilon_2)/2$, where ϵ_h is the dielectric constant of the host and ϵ_1 and ϵ_2 are the real and imaginary parts for the metal. © 2006 American Institute of Physics. [DOI: 10.1063/1.2358209]

In recent years considerable research has gone into the study of all-optical switching devices for photonic applications, where the requirement of the material had been a large n_2 (nonlinear refractive index), low index change due to thermal effects, and small two-photon absorption (TPA).^{1,2} Furthermore, there is significant interest in using nanocomposites comprising of metal nanoparticles in dielectric host for such applications because of their nonlinear response³⁻⁵ and because of their potential use in applications below the diffraction limited regime.⁶⁻⁸ However, the selection of the metal-host system for a given application must be based on a careful evaluation of the key physical limitations in the interaction of light with matter. In this regard, there are two well accepted limitations. The first is the refractive index change due to thermal effects arising from light-matter interactions.¹ The second, which has been recognized as the ultimate limit for optical switching, is TPA.⁹ However, there has been no effort to combine these effects into a figure of merit describing the metal nanocomposite material in photonic applications involving optical modulation.¹⁰

In this letter we define a compound figure of merit (FOM_C) as the product of the thermal FOM (FOM_{therm}) and the TPA FOM (FOM_{TPA}). The reason for choosing the product as compared to a linear combination comes from the strong correlation between the TPA and thermal effects. In general, material having large TPA shows small linear absorption and thermal effects and vice versa. Therefore, it is difficult to select materials for such applications based simply on the linear combination of the two effects. A common example of a similar definition is that of the gain-bandwidth product used to optimize an operational amplifier.

The theoretical behavior for Ag, Au, and Cu nanoparticles embedded in an SiO_2 matrix was evaluated based on this FOM. The behavior of the FOM_C , which is device independent, shows that an extremely large value results at a specific combination of the metal and host dielectric function given by $\epsilon_h = (\epsilon_1 - \epsilon_2)/2$, where ϵ_h is the dielectric constant of the host and ϵ_1 and ϵ_2 are the real and imaginary parts of the

dielectric constant of the metal. These results could simplify the process of materials selection for nanocomposites in photonic switching applications at desired wavelengths.

We start with the criteria that conventional all-optical switching devices are based on generation of light induced phase shifts of the order of $p\pi$, where $4 \geq p \geq 1$ for a range of devices. The design in mind for these calculations is a Mach-Zehnder interferometer, where $p=1$, and the criterion for switching is given by⁷

$$p\pi = \frac{2\pi n_2 I_0 L}{\lambda}, \quad (1)$$

where I_0 is the switching intensity, L is the length of the device, and λ is the wavelength. Our first figure of merit requires that the thermal index change be a small fraction of the fast light-induced change ($n_2 I_0$).¹ The thermal index change can be expressed by

$$\text{thermal index change} = \frac{\partial n}{\partial T} \frac{\Delta Q}{C_p \rho V}, \quad (2)$$

where $\partial n / \partial T$ is the thermo-optic coefficient, C_p is the specific heat, V is the volume of the material heated by the light, ρ is the density of the material, and ΔQ is the energy absorbed by the material per pulse, which is given by

$$\Delta Q = \alpha L I_0 A \tau, \quad (3)$$

where A is the cross sectional area of the device, α is the linear absorption coefficient, and τ is the duration of the switching pulse. By using Eqs. (2) and (3) the FOM_{therm} becomes

$$FOM_{\text{therm}} = \frac{n_2 C_p \rho}{(\partial n / \partial T) \tau \alpha}. \quad (4)$$

Two-photon absorption can reduce the device throughput even if the linear absorption is small. A general criterion for this was developed by Stegeman *et al.*² based on Eq. (1) and the two photon absorption coefficient β as $\beta \lambda / 2n_2 < 1$ or $2n_2 / \beta \lambda > 1$.

Based on this, we defined our next figure of merit to be

^{a)}Electronic mail: hgarcia@siue.edu

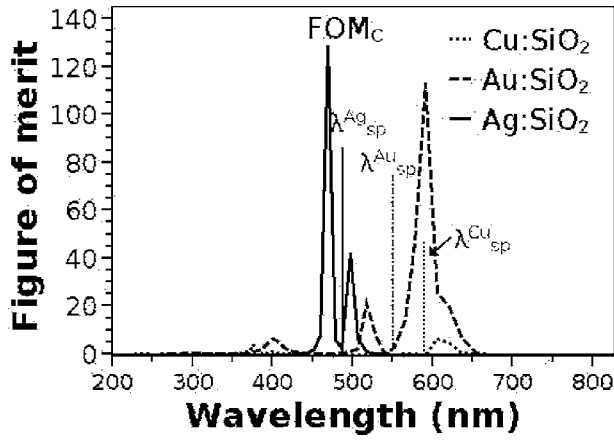


FIG. 1. Total figure of merit given by Eq. (14) for Ag (solid line), Au (dashed line), and Cu (dotted line) embedded in SiO_2 matrix. The wavelengths corresponding to the surface plasmon wavelengths are also indicated for each metal.

$$\text{FOM}_{\text{TPA}} = \frac{2n_2}{\beta\lambda}. \quad (5)$$

The compound figure of merit in this letter takes into account the switching limitations due to thermal heating and large two-photon absorption, and is defined as the product of Eqs. (4) and (5) to give

$$\text{FOM}_C = \text{FOM}_{\text{therm}} \text{FOM}_{\text{TPA}} = \frac{2n_2^2 C_p \rho}{\alpha \tau \beta \lambda (\partial n / \partial T)}. \quad (6)$$

Using this definition, an *attractive combination* of metal-dielectric would be one with a large value of the FOM_C . Using this new FOM_C , we evaluated the response for metal nanocomposites. In these structures we have a lot of freedom in choosing and controlling α , β , and n_2 , which are the only free parameters in the above figure of merit. In the evaluation we assumed the following.

- (1) ρ , C_p , and $\partial n / \partial T$ can be considered to be properties of the host only and are not influenced by the presence of the metal nanostructures (i.e., *dilute limit approximation*).
- (2) β , α , and n_2 are drastically modified by dielectric confinement, and they may be analyzed within the context of Mie theory.¹¹
- (3) The particle diameters are such that quantum confinement effects due to intraband dipole electronic transitions are negligible.
- (4) The main contribution to the nonlinear susceptibility comes from the interband electric dipole transition, and the contribution is negative and purely imaginary.

With the above assumptions we calculated FOM_C [Eq. (6)] for a metal nanocomposite by noting the following:

$$\frac{n_2}{\beta\lambda} = \frac{\text{Re}[\chi_{\text{eff}}^{(3)}]}{4\pi \text{Im}[\chi_{\text{eff}}^{(3)}]}, \quad (7)$$

where we have ignored, for the moment, the frequency dependence of the nonlinear susceptibilities. $\chi_{\text{eff}}^{(3)}$ is the effective nonlinear susceptibility and is given in the context of Mie's theory by

TABLE I. Substrate properties used in calculation of the FOM.

Substrate parameters	Value
Specific heat capacity C_p ($\times 10^6$ ergs/g K)	7.4
Density ρ (g cm^{-3})	2.33
Thermo-optic coefficient $\partial n / \partial T$ ($\times 10^{-6}$ K^{-1})	0.55
Refractive index n_0	1.46
Host dielectric constant ϵ_h	3.82

$$\chi_{\text{eff}}^{(3)} = \nu f_1^2 |f_1|^2 \chi_m^{(3)}, \quad (8)$$

where ν is the volume fraction of the metal in the host matrix, $\chi_m^{(3)}$ is the third order susceptibility of the metal cluster, and f_1 is an enhancement factor produced by the dielectric confinement, which can be expressed as

$$f_1 = \frac{3\epsilon_h}{\epsilon_1 + i\epsilon_2 + 2\epsilon_h}, \quad (9)$$

where ϵ_h is the real dielectric constant of the host and ϵ_1 and ϵ_2 are the real and imaginary dielectric constants of the metal nanoparticles, respectively. Using Eqs. (8) in (7) and using assumption #4 we get for the ratio of the real and imaginary parts in Eq. (7),

$$\frac{\text{Re}[\chi_{\text{eff}}^{(3)}]}{\text{Im}[\chi_{\text{eff}}^{(3)}]} = - \frac{\text{Im}[f_1^2]}{\text{Re}[f_1^2]}. \quad (10)$$

We calculated the ratio of n_2 (Ref. 12) and α (Ref. 4) using the following definitions:

$$\alpha = \frac{\nu \omega |f_1|^2 \epsilon_2}{n_0 c} \quad (11)$$

and

$$n_2 = \frac{12\pi}{n_0^2 c} \text{Re}[\chi_{\text{eff}}^{(3)}] = \frac{12\pi}{n_0^2 c} \nu |f_1|^2 \text{Re}[f_1^2 \chi_m^{(3)}], \quad (12)$$

where n_0 is the refractive index, c is the velocity of light, and ω is the frequency of the incident light. This results in a ratio of

$$\frac{n_2}{\alpha} = \frac{6\lambda |\chi_m^{(3)}|}{n_0 c \epsilon_2} \text{Re}[if_1^2]. \quad (13)$$

By using the above result and Eq. (9) in Eq. (6) we get the compound FOM as

TABLE II. Material properties for the metals used in the calculation of the FOM.

Metal parameters	Ag	Au	Cu
Fermi velocity v_F ($\times 10^8$ m/s)	1.42	1.4	1.28
Electron density ρ_e ($\times 10^{22}/\text{cm}^3$)	5.85	5.9	8.45
Effective mass m_{eff}	$0.96m_0$	$0.99m_0$	$0.99m_0$
High frequency dielectric constant ϵ	5.3	8.6	9.3
Radius and interparticle spacing (nm)	35, 75	35, 75	35, 75

TABLE III. Values of the wavelengths corresponding to the surface plasmon resonance (λ_{sp}) and strongest peaks in the FOM_{therm} (λ_{therm}), FOM_{TPA} (λ_{TPA}), and FOM_C (λ_C). The position of the strongest peak as predicted by the crude Drude model is expressed as λ_{FOM}^{drude} .

Metal	λ_{sp} (nm)	λ_{therm} (nm)	λ_{TPA} (nm)	λ_C (nm)	λ_{FOM}^{drude} (nm)
Ag	487	450	472	509	497
Au	552	583	550	591	560
Cu	591	618	618	607	606

$$FOM_C = \frac{108C_p \rho |\chi_m^2|}{\pi \tau (\partial n / \partial T) n_0} \times \left\{ \frac{\lambda \epsilon_2 \epsilon_h^2 (\epsilon_1 + 2\epsilon_h)^2}{[(\epsilon_1 + 2\epsilon_h)^2 - \epsilon_2^2][(\epsilon_1 + 2\epsilon_h)^2 + \epsilon_2^2]} \right\}. \quad (14)$$

The dependence of the FOM_C on the dielectric constants has been put in the brackets. As would be expected, this FOM_C goes to zero under the highly absorbing conditions found at the plasmon resonance condition of $\epsilon_1 + 2\epsilon_h = 0$. On the other hand, as Fig. 1, large maxima are observed in the wavelength range for the various metals using the parameters from Table I and Table II. The large maxima occur at the condition of $(\epsilon_1 + 2\epsilon_h)^2 - \epsilon_2^2 = 0$. The wavelengths corresponding to these maxima for each metal are tabulated in Table III and are compared to nearby peak positions in the FOM_{therm} and FOM_{TPA} . A significant difference in wavelength of the FOM_C to those in the thermal or TPA cases is observed. This difference is especially important when put in the context of data communication bandwidths, where wavelength separations of 1–5 nm are routine. The physical origin of these wavelengths can be understood by analyzing the location of the peaks within the framework of the simplifying Drude model. In this model the real and imaginary components of the dielectric susceptibility of the metal in the high frequency limit ($\omega \tau \gg 1$) are given by $\epsilon_1 = \epsilon_0 - \omega_p^2 / \omega^2$ and $\epsilon_2 = \omega_p^2 / \omega^2 \tau$, where ϵ_0 is the contribution to the dielectric constant of the metal from bound charges and ω_p is the bulk plasmon resonance of the metal. Using the condition for the FOM_C maxima and the condition for surface plasmon resonance given by $\omega^2 / \omega_{sp}^2 = \epsilon_1 + 2\epsilon_h$.

After some algebraic manipulation, the frequency ω_{FOM} at which the maxima in the FOM_C occurs can be related to the surface plasmon frequency ω_{sp} by the expression

$$\left(\frac{1}{\omega_{sp}^2} - \frac{1}{\omega_{FOM}^2} \right)^2 = \left(\frac{1}{\omega_{FOM}^3 \tau} \right)^2. \quad (15)$$

In Eq. (15), the quantity on the right side is always positive but the quantity on the left side can be positive or negative giving

$$\frac{\omega_{FOM}^2}{\omega_{sp}^2} = \left(1 \pm \frac{1}{\omega_{FOM} \tau} \right). \quad (16)$$

Therefore we find that the maxima in the FOM_C can be located above or below the surface plasmon resonance. In the evaluation of Eq. (14) we have chosen the positive values obtained from the above expression. In Table III we have also indicated λ_{FOM}^{drude} estimated using the above Drude model for the various metals using experimental values for λ_{sp} and the relaxation times from Ref. 13. It is apparent that this crude model also predicts a shift in the peak position from

λ_{sp} , λ_{therm} , and λ_{TPA} and actually predicts very well the λ_{FOM} position for the case of Cu estimated from Eq. (14).

Recently there have been reports of lasing of Au nanoparticles in water.¹⁴ We estimated a surface plasmon resonance for their Au-water system to be at 700 nm, while the observed lasing occurred with various peaks located at 720 nm or higher. Using our model, we have estimated that the FOM_C achieves a maximum for Au nanoparticles in water at 720 nm for an electron relaxation time of 9.3×10^{-15} s. While this may be rather coincidental, it should be emphasized that the FOM_C expressed by Eq. (14) represents a situation where losses are minimized and the nanoparticles act as excellent scattering centers.

In conclusion, we have defined a compound figure of merit FOM_C for metal-dielectric nanocomposites that takes into account limitations to optical switching from thermal index changes and two-photon absorption. As expected the FOM_C is zero at the plasmon resonance when large absorption occurs but has extremely large values at a value of frequency which is dependent only upon the dielectric constants of the metal and dielectric. This result could allow the rapid selection of a metal-host system for operation at a desired wavelength.

One of the authors (R.K.) acknowledges support by the National Science Foundation through Grant No. DMI-0449258.

¹S. R. Friberg and P. W. Smith, IEEE J. Quantum Electron. **23**, 2089 (1987).

²G. I. Stegeman, E. M. Wright, N. Finlayson, R. Zanonc, and C. T. Seaton, J. Lightwave Technol. **6**, 953 (1988).

³L. Yang, Ph.D. thesis, Vanderbilt University, 1993.

⁴L. Yang, D. H. Osborne, R. F. Haglund, Jr., R. H. Magruder, C. W. White, R. A. Zuhr, and H. Hosono, Appl. Phys. A: Mater. Sci. Process. **62**, 403 (1996).

⁵W. T. Wang, Z. H. Chen, G. Yang, D. Y. Guan, G. Z. Yang, Y. L. Zhou, and H. B. Lu, Appl. Phys. Lett. **83**, 1983 (2003).

⁶R. F. Haglund, Jr., Mater. Sci. Eng. **253**, 275 (1988).

⁷S. Maier, P. Kik, H. Atwater, S. Meltzer, E. Harel, B. Koel, and A. Requicha, Nat. Mater. **2**, 229 (2003).

⁸J. H. Huter and E. Fendler, Adv. Mater. **16**, 1685 (2004).

⁹V. Mizrahi, K. W. DeLong, G. I. Stegeman, M. A. Saifi, and M. J. Andrejco, Opt. Lett. **14**, 1140 (1989).

¹⁰E. Hartfield and B. Thompson, *Handbook of Optics* edited by W. G. Driscoll and W. Vaughan (McGraw-Hill, New York, 1978), Chap. 17, pp. 17–1–17–24.

¹¹M. Born and E. Wolf, *Principles of Optics* 6th ed. (Pergamon, New York, 1980), 633–647.

¹²R. L. Sutherland, *Handbook of Nonlinear Optics* (Dekker, New York, 1996), pp. 295–384.

¹³P. B. Johnson and R. W. Christy, Phys. Rev. B **6**, 4370 (1972).

¹⁴J. Kang and J. Khurgin *Conference on Lasers and Electro-Optics/Quantum Electronics and Laser Science and Photonic Applications, Systems and Technologies* (Optical Society of America, Long Beach, CA, 2006), Paper No. QTuI2.